Giovanna Concu, Nicoletta Trulli,
Direct and semi-direct ultrasonic testing for quality control of FRC-concrete adhesion,
Structures, Volume 32, 2021, Pages 54-64,
ISSN 2352-0124,
https://doi.org/10.1016/j.istruc.2021.02.061.
(https://www.sciencedirect.com/science/article/pii/S2352012421001727)
Abstract: Externally bonded Fiber Reinforced Composite (FRC) materials, such as Fiber Reinforced Polymers (FRP) and Fiber Reinforced Cementitious Matrix (FRCM), have been increasingly used over the last decades for retrofitting existing structural elements due to their excellent mechanical and physical properties. However, the effectiveness of the reinforcement depends on the quality of the adhesion between the reinforcement and its substrate. The present paper reports the results of an experimental campaign in which the Ultrasonic Pulse Velocity (UPV) testing has been applied to detect the presence of adhesion defects at the interface FRC-concrete. UPV has been carried out on concrete specimens strengthened with different types of FRC. Some inclusions have been specifically placed at the interface between the reinforcement and the concrete to simulate adhesion defects. UPV has been applied both in the direct and in the semi-direct mode, to simulate different realistic on-site situations, including the possible inaccessibility of some parts of the element to check. Results show that UPV, applied by means of both direct and semi-direct modes, allows to identify the presence of adhesion defects, and evoke the possibility of discriminating between different defects.
Keywords: Fiber reinforced concrete; Adhesion defects; Non destructive testing; Ultrasonic Pulse Velocity; Direct transmission; Semi-direct transmission

Direct and semi-direct ultrasonic testing for quality control of FRC-concrete adhesion

Giovanna Concu[1] and Nicoletta Trulli[1]

[1] Department of Civil and Environmental Engineering and Architecture, Cagliari 09123, Italy.

Correspondence author: Giovanna Concu; gconcu@unica.it

Abstract

Externally bonded Fiber Reinforced Composite (FRC) materials, such as Fiber Reinforced Polymers (FRP) and Fiber Reinforced Cementitious Matrix (FRCM), have been increasingly used over the last decades for retrofitting existing structural elements due to their excellent mechanical and physical properties. However, the effectiveness of the reinforcement depends on the quality of the adhesion between the reinforcement and its substrate. The present paper reports the results of an experimental campaign in which the Ultrasonic Pulse Velocity (UPV) testing has been applied to detect the presence of adhesion defects at the interface FRC-concrete. UPV has been carried out on concrete specimens strengthened with different types of FRC. Some inclusions have been specifically placed at the interface between the reinforcement and the concrete to simulate adhesion defects. UPV has been applied both in the direct and in the semi-direct mode, to simulate different realistic on-site situations, including the possible inaccessibility of some parts of the element to check. Results show that UPV, applied by means of both direct and semi-direct modes, allows to identify the presence of adhesion defects, and evoke the possibility of discriminating between different defects.

Keywords: Fiber reinforced concrete; Adhesion defects; Non Destructive Testing; Ultrasonic Pulse velocity; Direct Transmission; Semi-direct Transmission.

1. Introduction

Advanced Fiber Reinforced Composite (FRC) such as Fiber Reinforced Polymers (FRP) and Fiber Reinforced Cementitious Matrix (FRCM) have been increasingly used in structural engineering for both existing and new buildings strengthening, repairing and retrofitting due to their remarkable strength and stiffness properties, excellent strength-to-weight and stiffness-to-weight ratios, high durability, high corrosion resistance [1-4]. There are many reasons for strengthening and upgrading civil structures: design and construction errors, damage caused by seismic loads and accidental actions, changes in functionality. However, the structural performance is strongly dependent on a proper application, and an almost perfect adhesion between FRC materials and the substrate must be granted to assure the effectiveness of the reinforcement. In light of this, the goal of testing the quality of FRC - substrate adhesion has become of great relevance, and special emphasis has been dedicated to the development of methods for analysing, studying and controlling its performance [5-8].

Quality control is an essential aspect not only for verifying the correct setup of fiber reinforced materials, but also for monitoring them during their service life. Indeed, the bond setup in the interface between FRP or FRCM and concrete substrate can be seriously compromised by air presence, inclusions or irregularities, caused by an incorrect application of the reinforced

system, or by gaps and voids generated following loads application and exposure to atmospheric agents.

The main advantage of Non Destructive Testing (NDT) methods is clearly their ability to non-invasively provide information on adhesion performance, hence in the past various NDT techniques have been proposed with this aim. Among NDTs, Acoustic Methods (AM), based on the analysis of elastic waves propagating through the material, are commonly applied for materials inspection and they are applied also for detecting the presence of subsurface anomalies or defects in elements strengthened with FRC. Bastianini et al. [9] used pulsed echo ultrasonic analysis for testing different type of composite materials applied to different substrates by using the amplitude of the ultrasonic signal. Mahmut et al. [10] performed an acousto-ultrasonic nondestructive testing for detecting and imaging the delamination between carbon fiber-reinforced polymer (CFRP) sheet and concrete substrate. Li et al. [11] used guided waves for identifying CFRP-reinforced concrete debonding. Mirmiran and Wei [12] used ultrasonic pulse velocity testing to quantify the extent and progression of damage in concrete filled FRP-tubes. Mahmoud et al. [13] utilized surface acoustic waves for non-destructive structural health monitoring of concrete specimens externally bonded with CFRP composites and subjected to accelerated aging conditions. Dugnani et al. [14] applied a cross-correlation electromechanical impedance–based approach for detecting adhesive bond-line degradation. La Malfa Ribolla et al. [15, 16] proposed an ultrasonic technique that couples the Akaike information criterion, used as automatic starting time signal detection, and the equivalent time-length of the signal, used as indicator of the energy distribution of the signal with respect to the beginning of the signal, for detecting delamination defects in FRP reinforcement. Concu et al. [17] applied pulse velocity ultrasonic testing for evaluating concrete strengthened with different kinds of FRP.

Despite the large amount of contributions and their valuable results, most of the studies on AM for FRC quality control involve the application of sophisticated methodologies, both in terms of instrumentation and, above all, in terms of processing and interpretation of experimental data, therefore the application of these methodologies on site is neither quick and simple nor within the reach of common operators who generally deal with the application and control of FRC. In addition, on-site quality control often requires tools and techniques able to adapt to specific situations, as in the case of inaccessibility of some parts of the element to check - beams, pillars, walls - therefore the study of techniques capable of providing information also in these cases is very useful. Among AM, a technique that meets these requirements is the Ultrasonic Pulse Velocity (UPV) method, a quite simple technique based on the measurement of the velocity of propagation of elastic waves in the material, widely spread and commonly used for on-site materials quality control. Several studies related to the application of UPV to concrete and reinforced concrete diagnostics can be addressed, the main topics being the evaluation of concrete early-stage properties [18-21], the assessment of physical and mechanical properties [22-29], the evaluation of damage [30-37].

UPV can be applied in different ways (direct, semi-direct and non-direct transmission), depending on the possibility to access to the structural element. In particular, the semi-direct mode can be used when the element is accessible only on two adjacent sides, and, although it is normally considered less reliable than the direct mode [38], it can often be the only suitable choice of using UPV on site. As evidence of the interest aroused by the possible use of UPV semi-direct technique in materials diagnostics, the literature presents a number of studies on this topic. Turgut and Kucuk [39] conducted an experimental study to compare direct, non-direct and semi-direct UPV measurements on concrete blocks coming from different mix

batches and having different cube compressive strength. Bui et al. [40] applied two types of configurations, the non-direct and the semi-direct transmission, to cement base samples at different levels of damage generated by freeze-thaw cycles. Benaicha et al. [41] applied the direct, semi-direct and non-direct transmission modes to non-destructive evaluation of the curing degree of fiber-reinforced concrete. Andi et al. [42] analysed the correlation between UPV direct, semi-direct and non-direct measurements in concrete specimens. Ndagi et al. [43] reviewed the UPV test by considering different arrangement options and common factors that affect the results. Ivanchev and Slavchev [44] determined the compressive strength and modulus of elasticity of concrete using UPV direct, semi-direct and non-direct transmission ways. Saleem [45] focused on the use of ultrasonic pulse velocity to study the degradation in steel-concrete bond subjected to increasing loading using both direct and semidirect testing methods.

To the knowledge of the authors, there are no in-depth studies on the application of UPV for the quality control of the adhesion between FRC and substrate. For this reason, an experimental test has been run with the purpose of checking the efficacy of UPV in detecting anomalies at the interface between FRC and concrete. To this end, UPV has been carried out on thirty concrete specimens strengthened with three different types of FRC. Some inclusions have been specifically placed at the interface between the reinforcement and the concrete to simulate adhesion defects. UPV has been applied both in the direct and in the semi-direct mode, to simulate different realistic on-site situations, including the possible inaccessibility of some parts of the element to check. Preliminary results point out the possibility to extend the use of this relatively cheap, fast, and widespread method for quick control of FRC-concrete interface.

2. Materials

The experimental tests have been carried out on thirty beams 0.15x0.15x0.6m made of concrete C30/37 [46] (Fig. 1 left). The locations where applying the transducers for UPV, three for each lateral face of specimens, have been marked (Fig. 1 right). These points lie on the centre line of each face, are 0.15 m apart from each other and from the edge of the base faces and have been marked with progressive numbering from 1 to 3 following the same direction for all faces.

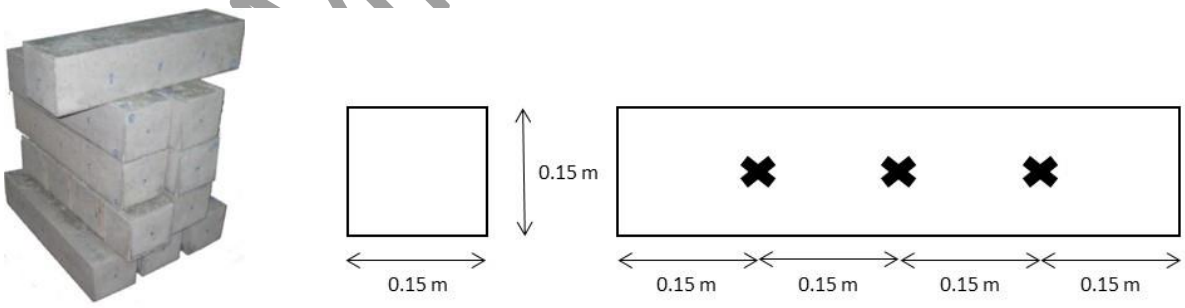

Figure 1. Concrete specimens (left). UPV measurements points (right).

Table 1. Main mechanical properties of the strengthening fibers (from manufacturer).

	Ruredil X Lam 50S	Ruredil X Wrap 310	Ruredil XMesh Gold
Tensile strength (MPa)	>2200	4800	5800
Tensile modulus of elasticity (GPa)	165	240	270

Ultimate elongation (%)	1.3	2	2.15

The strengthening systems were provided by Ruredil and were of three types: FRP lamina, FRP sheet and FRCM sheet. The physical and mechanical properties of the strengthening fibers were provide by the manufacturer and are reported in Table 1.

Each type of reinforcement was applied on 10 specimens, thus identifying 3 groups of reinforced specimens called group A, group B, and group C. For each group, perfect adhesion between the reinforcement and the substrate was sought on two specimens, while adhesion defects were simulated on the remaining eight specimens, placing on the lateral face, where the reinforcement was then applied, three types of artificial defects: Teflon element (T), accumulation of glue (G), and plastic element (P) (see Fig. 2 and Table 2). These defects were chosen to simulate some common errors in FRC application: Teflon simulates the lack of adhesion between the FRC and the substrate [11, 15, 16], the accumulation of glue simulates the variation of the thickness of the glue layer [9], plastic simulates the presence of an inclusion of a material different from the FRC and the substrate. The defects were glued to concrete by means of a bicomponent epoxy resin.

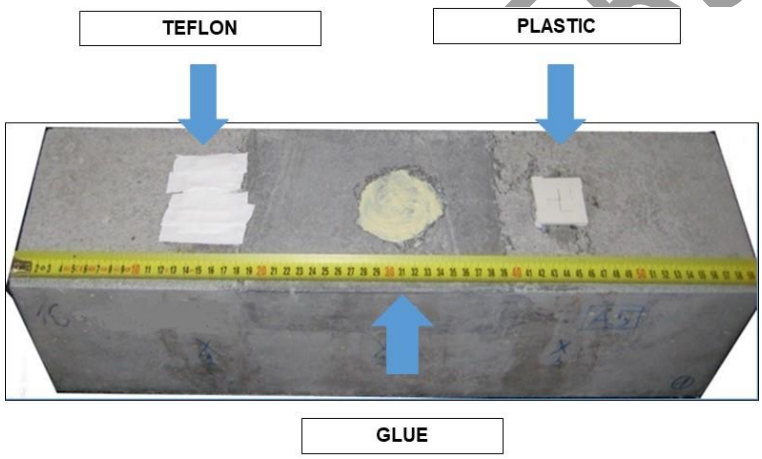

Figure 2. Artificial adhesion defects: Teflon (left), Glue (centre), Plastic (right).

Table 2. Defects.

Defect	Shape	Plan size (m)
Teflon (T)	rectangular	0.04x0.06
Glue (G)	round	0.04
Plastic (P)	square	0.03

Table 3 shows the schematic of the groups of specimens and the adhesion defects, whereas Figure 3 shows some steps of the strengthening process. The application of the reinforcement systems involved different phases: i) homogenization of the concrete substrate, ii) application of bicomponent epoxy resin, iii) application of the FRC lamina or sheets, iv) impregnation of the reinforcement system, v) application of a second layer of resin in case of the FRP sheets.

Table 3. Specimens, reinforcements, and defects.

Group	Reinforcement	Specimen	Defect
A	FRP lamina (Ruredil X Lam 50S)	A1, A2	-
		A3-A10	T, G, P
B	FRP sheet (Ruredil X Wrap 310)	B1, B2	-
		B3-B10	T, G, P
C	FRCM sheet (Ruredil XMesh Gold)	C1, C2	-
		C3-C10	T, G, P

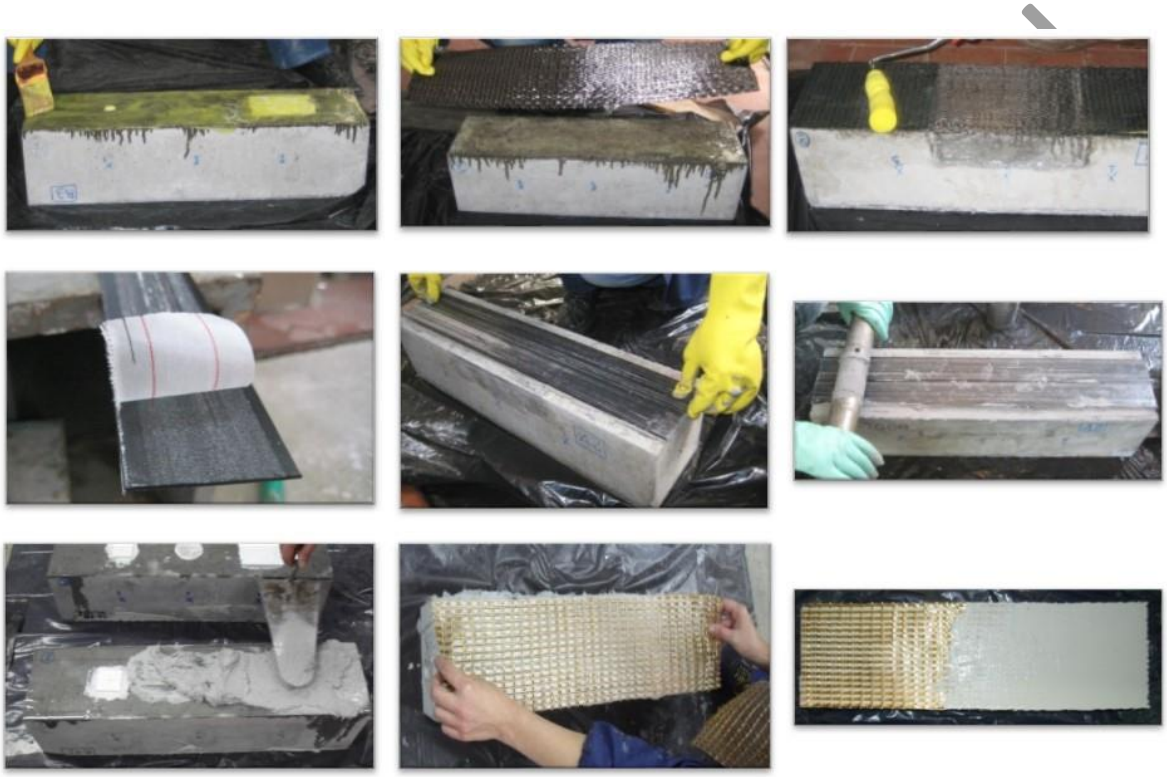

Figure 3. Strengthening process. FRP lamina (up), FRP sheet (center), FRCM sheet (down).

3. Ultrasonic Pulse Velocity Testing

Ultrasonic testing methods consist in the study of the propagation of elastic waves within the material. The most widespread way of applying ultrasonic testing for materials diagnostics is based on the measurement of the velocity V of longitudinal waves propagating through the material, thus performing the so-called Ultrasonic Pulse Velocity (UPV) testing. A characteristic of the method is that it considers the overall mechanical properties of the material [47].

3.1.Theoretical model

When a material is modified by means of an elastic vibration, the perturbation propagates in it in a certain time in the form of an acoustic wave originating from the vibration of the particles that make up the material. As for all wave phenomena, it is possible to define the wavelength λ, the period T, and the frequency f, quantities linked together by the relationship:

$$V = \lambda / T = \lambda \cdot f \quad (1)$$

where V represents the velocity of the acoustic wave in the material. When the frequency exceeds the value of 20kHz, the acoustic wave is called ultrasonic wave.

The propagation of ultrasonic waves can take place in materials in different ways. Ultrasonic waves can propagate as a result of oscillations of the particles parallel to the direction of the wave front motion (longitudinal waves) or perpendicular to it (transverse waves). These are the waves most frequently used for UPV of on-site structures and construction materials. The ultrasonic waves propagate in the materials under the influence of a local pressure P, which represents the pressure variation the particles undergo when the wave passes, evaluated with respect to a static equilibrium value. According to the pressure variation and the oscillation velocity ξ of the particles, the acoustic impedance Z of the material is defined by the following relationship:

$$Z = P / \xi \quad (2)$$

and when the propagation occurs without phase shift between P and ξ, then Z can be expressed as a function of the physical properties of the material by means of the expression:

$$Z = d \cdot V \quad (3)$$

where d is the density of the material and V is the propagation velocity of the wave. Z can be considered as a local characteristic of the material and expresses its resistance to wave propagation. When an ultrasonic wave impacts a surface or inhomogeneity, complex changes can occur that modify the motion of the particles due to Z differences of the materials involved. The incident wave undergoes transmission, reflection, and refraction phenomena according to the following values of transmission coefficient t and reflection coefficient r:

$$t = 4Z_2 / (Z_2+Z_1)^2 \quad (4)$$

$$r = (Z_2-Z_1)/(Z_2+Z_1) \quad (5)$$

where Z_1 and Z_2 are the acoustic impedances of the materials involved. The incident, transmitted, reflected, and refracted waves follow the Snell's low:

$$\sin\alpha_1/\sin\alpha_2 = V_1/V_2 \quad (6)$$

where α_1 and α_2 identify the direction of the waves propagating in materials 1 and 2, and V_1 and V_2 are the velocity of propagation of waves in materials 1 and 2. From the foregoing considerations, it follows that the variation of V can provide indications that the ultrasonic beam has run into discontinuities along its path, therefore V is a parameter widely used in the diagnostics of materials.

During the passage through the material, the ultrasonic waves also undergo attenuation phenomena caused essentially by absorption and scattering. Scattering, which occurs whenever waves impact particles of a size comparable with their wavelength, results in the overall deviation of part of the incident waves from the original path. A further cause for energy loss is intrinsic to the way waves are generated by the transducer. In fact, the beam of ultrasonic waves generated by a probe is divergent, and this involves a progressive reduction of the energy

associated with the wave as the distance from the source increases. The intensity of the ultrasonic waves inside the beam generated by the transducer is not constant but varies due to the finite dimensions of the source which give rise to diffraction phenomena. Although the representation of the emitted ultrasonic beam is rather complex, a commonly accepted simplified schematic is shown in Figure 4.

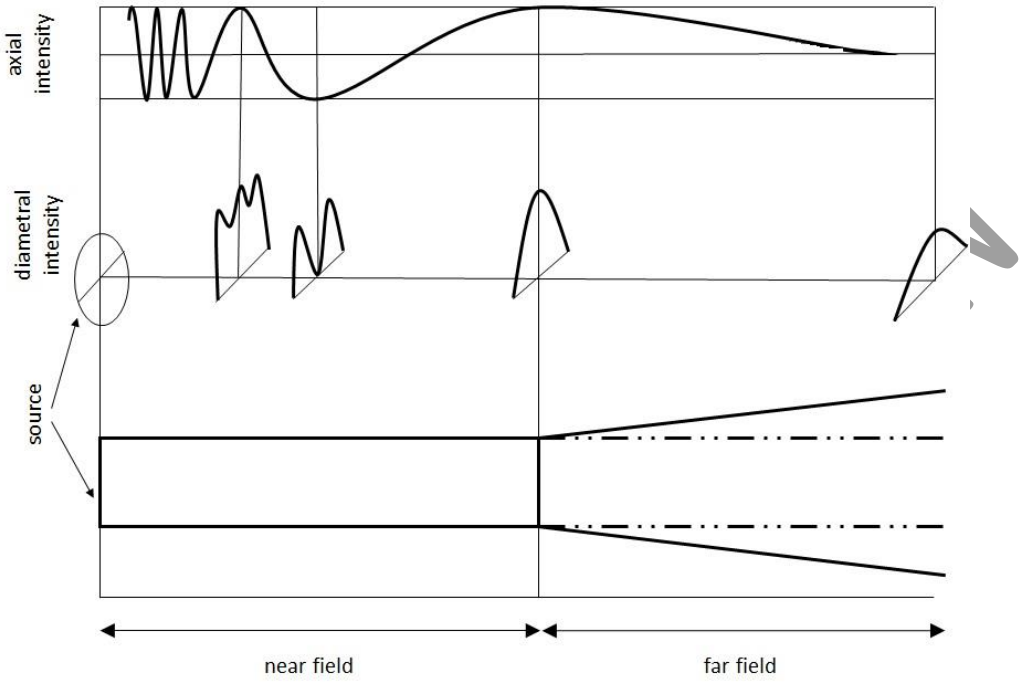

Figure 4. Emitted ultrasonic beam.

Assuming that the transducer is a cylinder with a certain diameter, the ultrasonic beam appears characterized by a first zone, called near field or Fresnel zone, in which the intensity is fluctuating between a minimum and a maximum value; the length of the near field increases with increasing wave frequency and transducer diameter. Beyond the near field, the ultrasonic beam becomes more uniform, and there is a tendency to diverge according to an angle inversely proportional to wave frequency and transducer diameter; this zone is called far field or Fraunhofer zone, and here the ultrasonic energy gradually decreases until it disappears. As shown in Fig. 4, in the far field there is a decrease in wave energy with increasing distance from the source, and for a given distance this decrease is minimal in the axial direction of the ultrasonic beam and increases towards the end of the emission cone, in which it is maximum. Therefore, if the detection of the waves is made in a different direction from the axial one in which the energy is maximum, the attenuation can be such as to affect the possibility to accurately detect the instant of arrival of the wave at the receiver placed at a certain distance from the source. For this reason, the standards relating to concrete UPV generally suggest the direct transmission mode, in which the source and the receiver are aligned along the ultrasonic beam axis and the energy associated with the wave is maximum.

When applied to concrete, UPV measures the velocity of propagation of the elastic waves, determined as the ratio between the distance between transmitter and receiver and the time taken to travel it according to the following equation [38]:

$$V = L/T \quad (7)$$

where V is the wave velocity, L is the path length, T is the time taken by the wave to travel the path.

It should be borne in mind that the elastic waves undergo, within the examined element, refractions and reflections, due to the presence of aggregates, cracks, voids. This entails an attenuation of the signal due to the absorption of energy, as previously illustrated. Furthermore, due to the effect of voids or cracks, the path actually made by the elastic waves can be longer than the distance between the transmitter and the receiver. The velocity calculated according to Eq. 7 may differ from the actual propagation velocity through the material. For this reason, the velocity calculated according to Eq. 7 is often called apparent velocity. As previously illustrated, although the direction in which the maximum energy propagates is along the ultrasonic beam axis, it is possible to detect waves which have travelled through the concrete in some other direction. It is therefore possible to make measurements of wave velocity by placing the two transducers on opposite faces (direct transmission DT), on adjacent faces (semi-direct transmission ST), or on the same face (indirect transmission IT) of the element (Fig. 5). In ST and IT modes, a lower precision than DT mode in the determination of the first arrival of the wave to the receiver is expected due to the greater attenuation, and this generally results in velocity values lower than those obtained with the DT. The ST is used when the DT cannot be used, for example, at the corners of structures, While IT is the least sensitive method, and should be used when only one face of the concrete is accessible, or when the quality of the surface concrete relative to the overall quality is of interest [38]. The IT sensitivity to the conditions of the superficial layer would lead to choose this mode to test the adhesion between the FRC and the underlying concrete. However, as highlighted by Annex A of [38] the IT arrangement involves some uncertainty regarding the exact length of the transmission path, since the areas of contact between transducers and concrete are of significant size, and therefore requires more complex measurements and data processing than DT and ST, which partially invalidates its ease of use and expedition. IT therefore belongs to the methods having greater complexity than those considered in the present paper, so the analysis of its effectiveness is to be considered out of the scope of this experimentation, in which only DT and ST are considered. For DT, the path length is the shortest distance between the transducers, whereas for ST it is generally found to be sufficiently accurate to take the path length as the distance measured from centre to centre of the transducer faces [38].

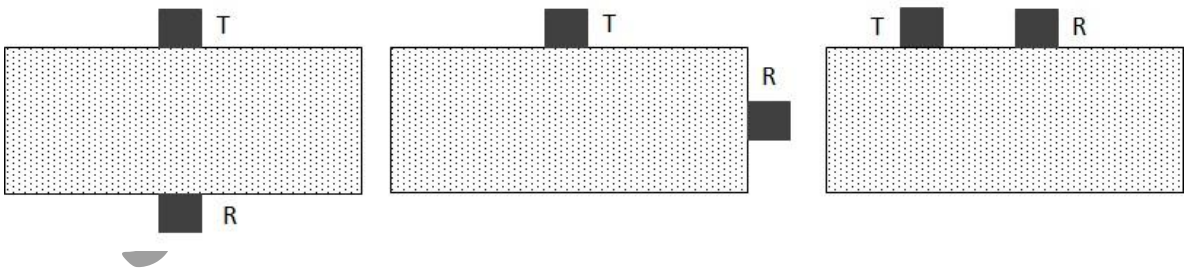

Figure 5. Direct transmission (left), Semi-direct transmission (centre), Indirect transmission (right). T = emitter transducer, R = receiver transducer.

The velocity V of longitudinal waves depends on the elastic constant of the material concerned through the following relation [48, 49]:

$$V = \sqrt{\left(\frac{E_d}{d}\right) \cdot \frac{(1-n)}{(1+n)\cdot(1-2n)}} \tag{8}$$

where E_d [kg/(m·s^2)] is the dynamic modulus of elasticity, n is the dynamic Poisson's number, d [kg/m^3] is the density, thus, the velocity V [m/s] can give information on the physical-mechanical condition of the materials. European Standard EN 12504-4 [38] suggests that the pulse velocity can be used for the determination of the uniformity of concrete, the presence of cracks or voids, changes in properties with time and in the determination of dynamic physical properties, and that it may also be used to estimate the strength of concrete elements on site or of specimens, although it is not intended as an alternative to the direct measurement of the concrete compressive strength. Standard [38] also recommends considering the factors that can influence the pulse velocity measurements: i) moisture content of the concrete, mainly dependent on the curing conditions, to be carefully considered when estimating strength; ii) concrete temperature, to be considered if outside the range 10°C-30°C; iii) path length over which the pulse velocity is measured, that should be long enough not to be significantly affected by the heterogeneous nature of the concrete; iv) shape and size of the specimen, that can be neglected as influencing factors unless the least dimension of the specimen is less than a minimum value suggested in [38], Annex B, as a function of transducers frequency. All these factors can be considered irrelevant with respect to the experimentation carried out, as the specimens underwent the same curing conditions until hardening, the temperature was within the safe range, the minimum path length (0.15 m) was not less than the limit proposed in [38] and the minimum dimension of the specimen (0.15 m) was higher than the limit (0.065 m) suggested by [38] for the transducers frequency used (54k Hz).

3.2.Experimental

The UPV has been carried out on the specimens before and after the reinforcement application applying both DT and ST, to evaluate its reliability in detecting adhesion problems and simulate different testing situations on site.

The testing equipment included:

- a Vellemann Instruments arbitrary waveform generator for signal generation,
- a Vellemann Instruments digital oscilloscope for signal visualization and preliminary analysis,
- a pair of piezoelectric transducers (54 kHz resonant frequency) for signal transmission and acquisition,
- a PC for data storage and signal processing.

The choice of the frequency of the transducers mainly depends on the need to avoid interference from the natural inhomogeneities of the concrete, namely the aggregates. Considering that the maximum diameter of specimens' aggregates was about 0.02 m, a wavelength equal to at least twice the diameter, and therefore equal to about 0.04 m, was chosen. A preliminary test carried out on specimens highlighted an expected propagation velocity of about 2000 m/s on average. By applying Equation 7, in which V is the expected velocity and L is the wavelength, a frequency f = 1/T of approximately 50 kHz is obtained. The 54 kHz frequency was therefore chosen, guaranteed by commercially available transducers.

Transparent Vaseline was used to couple transducers to specimens, to reduce signal energy dissipation due to different acoustic impedance between the material kept in contact. The measurement set-up and the operative procedure are shown in Figure 6.

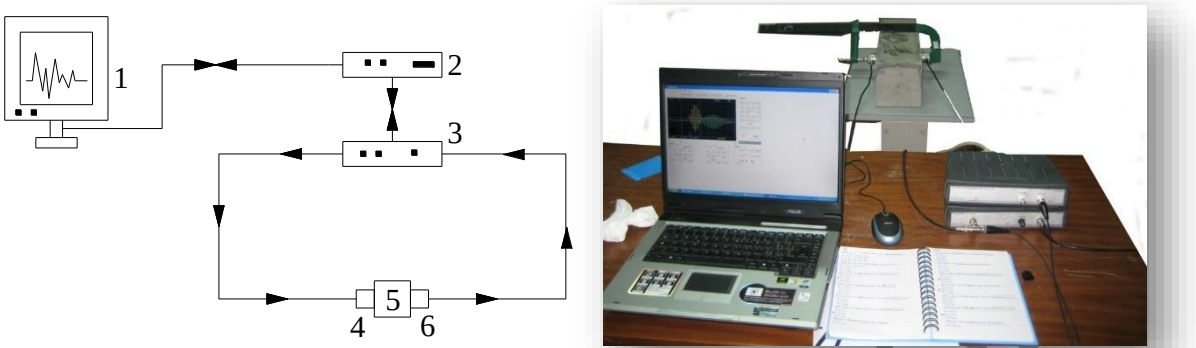

Figure 6. UPV set-up. 1) PC, 2) Signal generator, 3) Oscilloscope, 4,6) Transducers, 5) Specimen.

The excitation signal was a seven-and half-cycle tone burst enclosed in a Hanning window (Fig. 7), used to reduce the leakage phenomena in AM [50-52] and described by the following equation:

$$y(t) = \frac{1}{2} \cdot \sin(2\pi f t) \cdot \left[1 - \cos\left(\frac{2}{15} 2\pi f t\right)\right] \tag{9}$$

where f is the frequency of the starting sine wave.

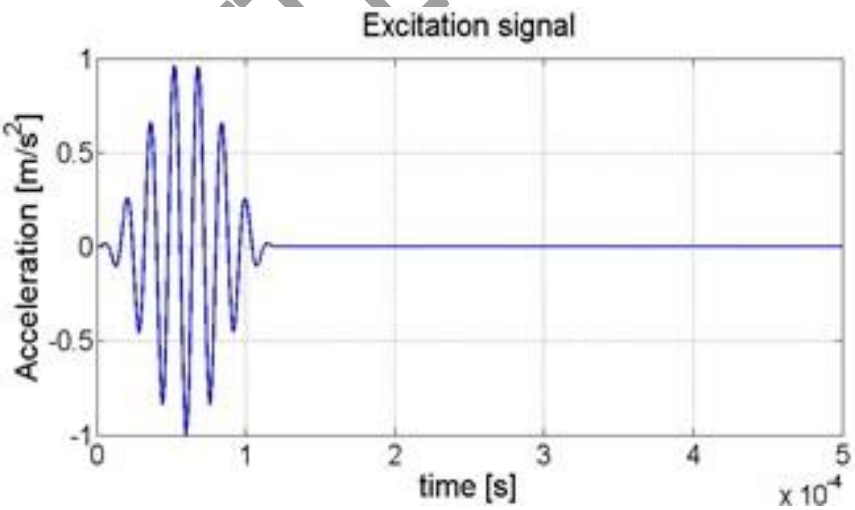

Figure 7. Excitation signal.

For each specimen, travel time T has been measured along selected paths of length L, different depending on whether DT or ST was applied (Fig. 8), and then propagation velocity V has been determined as the ratio L/T, as suggested by [38]. T is taken as the time that elapses between the first deflection of the trace of the signal emitted and that of the signal received (Fig. 9). The process of extracting the first arrival travel time of a wave can be cumbersome, especially when the waveform received is unclear, therefore various signal processing methods are proposed in

the literature to automate the process. However, automatic detection methods can be complex and unsuitable for fast UPV applications, therefore manual picking was used in this experimentation according to Boulay et al. [53], who commented that automatic methods are often ineffective and recommended manual picking.

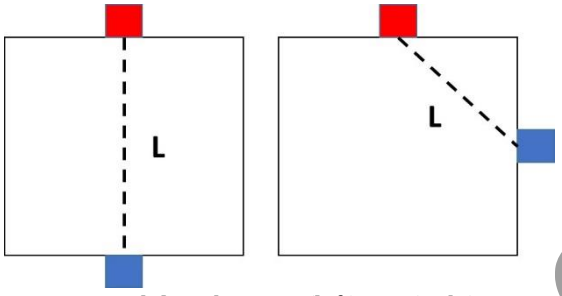

Figure 8. Path length L. DT (left), ST (right).

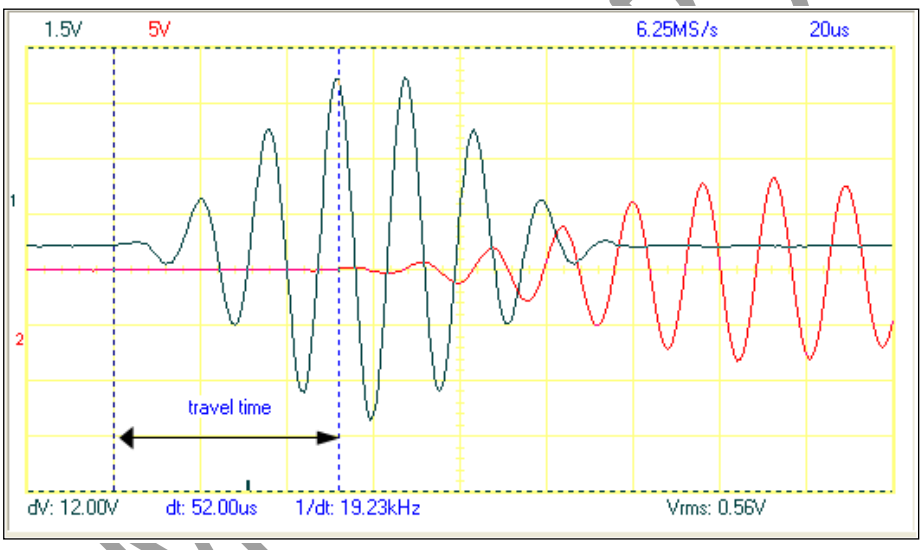

Figure 9. Measure of travel time T (emitted signal in green, received signal in red).

Figure 10 shows the measuring points and the related hypothetical paths of the signal in the case of DT and ST carried out before and after the application of the reinforcement. It is worth noting that in reinforced specimens the adhesion defects have been settled below the reinforcement in correspondence with the three positions of the emitter transducer, so in the measurements carried out after strengthening one end of the signal path always coincides with the position of the defect.

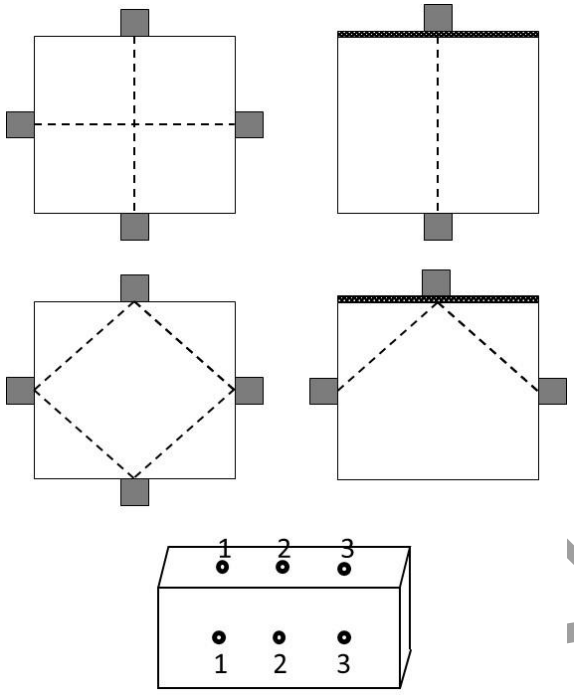

Figure 10. Scheme of the UPV measurements. DT (up) and ST (centre) before strengthening (left) and after strengthening (right). Three measurement points for each lateral face of the specimen (down).

4. Results and discussion

According to the UPV measurements scheme reported in Figure 10, on each specimen, six DT measurements and twelve ST measurements of V have been carried out before the application of the reinforcement, whereas after strengthening three DT measurements and six ST measurements have been carried out.

4.1.UPV of specimens without adhesion defects

Table 4 reports the results of UPV carried out on all specimens before strengthening and on specimens without artificial adhesion defects after strengthening.

Table 4. Velocity of propagation in reference specimens and in non-defective strengthened specimens. s = number of specimens, n = total number of measurements, Vm = average V, DS = standard deviation, CV = coeff. of variation, PD = percentage difference between DT and ST values.

	Before strengthening		FRP lamina strengthening		FRP sheet strengthening		FRCM sheet strengthening	
	DT	ST	DT	ST	DT	ST	DT	ST
s	30	30	2	2	2	2	2	2
n	180	360	6	12	6	12	6	12
Vm (m/s)	2814	2256	2765	2127	2538	2047	2646	2246
DS (m/s)	142	178	54	171	320	218	80	288
CV	0.05	0.08	0.019	0.080	0.126	0.107	0.30	0.128
PD (%)	27.4		29.9		23.9		17.8	

Regarding the tests on the specimens before strengthening, it can be observed that the data acquired via DT and via ST are little scattered, as can be seen both from the CV in Table 4 and from the distributions in Figure 11. Furthermore, the two sets of data, DT and ST, for which a percentage difference of about 27% can be calculated, are clearly distinguishable from each other, as illustrated in the scatter plot in Figure 12.

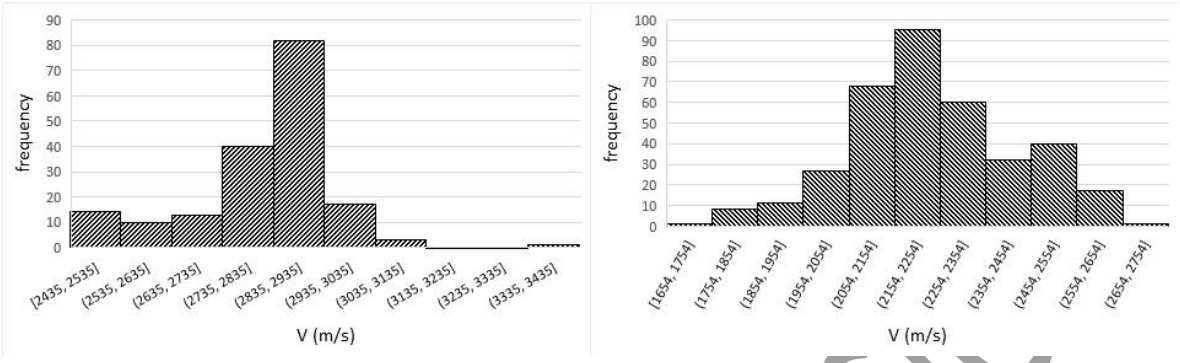

Figure 11. Distribution of V (m/s). DT measurements (left) and ST measurements (right).

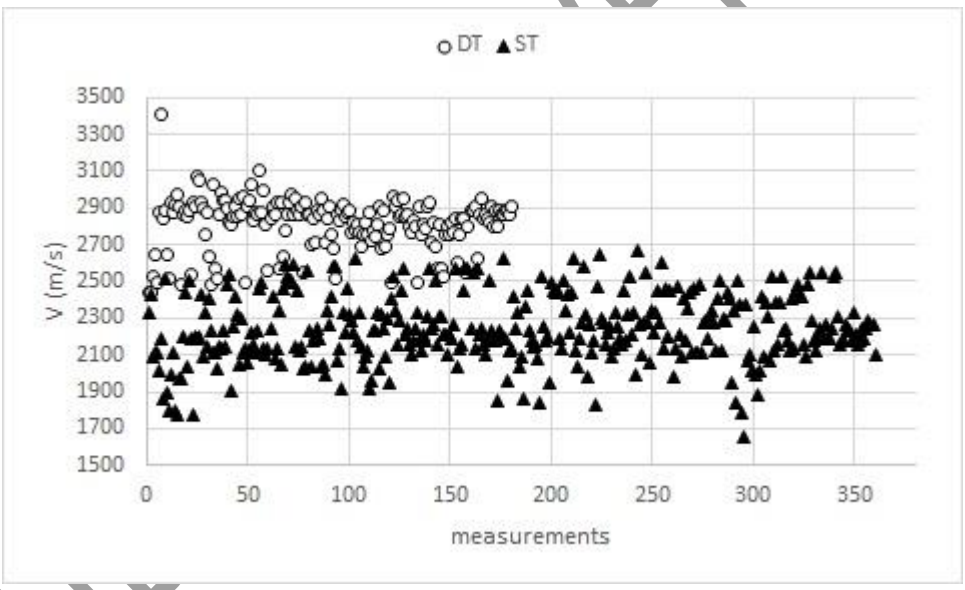

Figure 12. Scattering of V (m/s) data for DT and ST measurements.

This aspect is confirmed by the application of the Mann-Whitney U test, which allows to evaluate whether the two samples are extracted from one single population (null hypothesis) or not. Assuming a significance level p = 0.05, the Mann-Whitney U test compares the calculated U to the critical value U* below which the significance is less than 0.05. The Mann-Whitney U test applied to the two sets V (DT) and V (ST) gives $U = 688 < U^* = 32400$. This means that the two data sets are extracted from different populations with a probability higher than 95% and highlights how the two measurement methods provide results significantly different. This outcome, in line with literature findings, is consistent with the theoretical model illustrated in Section 3.1, and in particular with the fact that the increase in attenuation for measurements made in a direction other than the axial one affects the measurement of waves transit time and consequently leads to lower waves velocity.

Regarding the tests on specimens strengthened with the three types of reinforcement applied correctly without the insertion of artificial adhesion defects, it can be noted in Table 4 that the percentage difference between DT and ST measurements varies between about 18% and 30% depending on the reinforcement type. In the context of each measurement method (DT or ST), on the other hand, it can be observed that the three reinforcements do not have an appreciably different effect on V measurements. This can be seen from the plots in Figure 13, which show a partial overlap between V data, and is confirmed also in this case by the application of the Mann-Whitney U test, which gives the probability of rejecting the null hypothesis (Table 5).

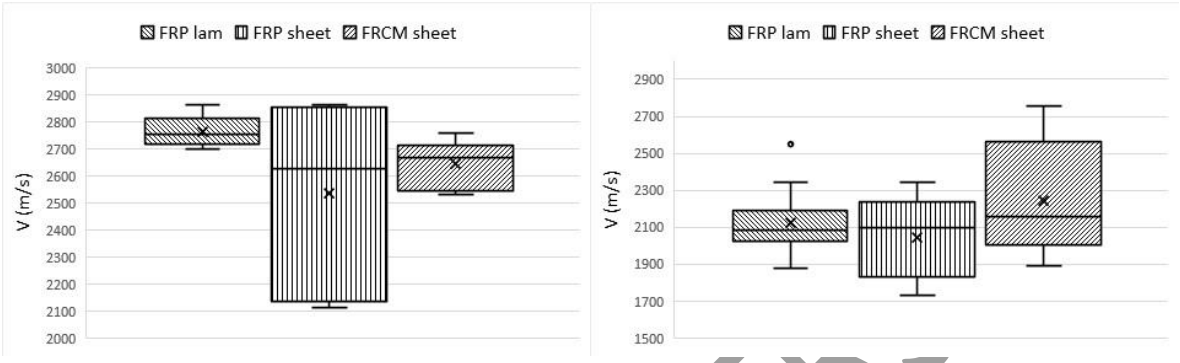

Figure 13. V (m/s) data in non-defective strengthened specimens. DT (left) and ST (right).

Table 5. Probability of rejecting the null hypothesis of Mann-Whitney U test for specimens with different reinforcements. Significance level p = 0.05. U is compared to critical value U* at p < 0 .05. U* = 5 for DT measurements and = 37 for ST measurements.

	FRP lamina vs FRP sheet		FRP lamina vs FRCM sheet		FRP sheet vs FRCM sheet	
	DT	ST	DT	ST	DT	ST
Mann-Whitney U test	15>5	61.5>37	3.5<5	58.5>37	18>5	47>37

It can be observed that the significance levels are close to but higher than the chosen limit value p = 0.05 in all cases except one in which U is slightly lower than the critical value. This outcome means that the three sets of V data (FRP lamina, FRP sheet, FRCM sheet) can be attributed to different populations with a probability of only 5% in all cases, except the one of FRP lamina vs FRCM sheet for which this probability is a bit higher. However, in any case, the null hypothesis, which states that the three samples are extracted from one single population, is prevalent.

4.2.UPV of specimens with adhesion defects

Table 6 reports the propagation velocity V in correspondence with the various defects as a function of the type of reinforcement, whereas Table 7 reports the results of UPV carried out on strengthened specimens with the artificial adhesion defects, along with V of the strengthened specimens with perfect adhesion assumed as reference. In view of the results previously commented (Table 5), the fact that different types of reinforcement were applied was not considered in Table 7 and subsequent analyses.

Table 6. Velocity of propagation along defective paths. Vm = average V, DS = standard deviation, CV = coeff. of variation.

	FRP lamina						FRP sheet						FRCM sheet					
	Teflon		Glue		Plastic		Teflon		Glue		Plastic		Teflon		Glue		Plastic	
	DT	ST	DT	ST	DT	ST	DT	ST	DT	ST	DT	ST	DT	ST	DT	ST	DT	ST
Vm (m/s)	1758	1360	2456	1766	2324	1718	1857	1406	2571	1856	2360	1716	1760	1652	2331	2071	2209	1915
DS (m/s)	299	178	135	156	278	286	339	146	166	149	199	175	151	381	98	295	139	392
CV	0.170	0.131	0.055	0.088	0.120	0.166	0.182	0.104	0.065	0.080	0.084	0.102	0.086	0.231	0.042	0.143	0.063	0.205

Table 7. Velocity of propagation in reference specimens and in defective specimens. s = number of specimens, n = total number of measurements, Vm = average V, DS = standard deviation, CV = coeff. of variation, ΔV= Vm decrease due to defects. The strengthening type is not considered.

	Reference specimens without defects		Adhesion defect: Teflon		Adhesion defect: Glue		Adhesion defect: Plastic	
	DT	ST	DT	ST	DT	ST	DT	ST
s	6	6	24	24	24	24	24	24
n	18	36	24	48	24	48	24	48
Vm (m/s)	2650	2140	1792	1502	2453	1905	2297	1763
DS (m/s)	214	245	261	305	161	264	209	360
CV	0.081	0.114	0.146	0.203	0.065	0.138	0.091	0.204
ΔV (%)	-	-	-32.38	-27.79	-7.43	-10.97	-13.30	-17.61

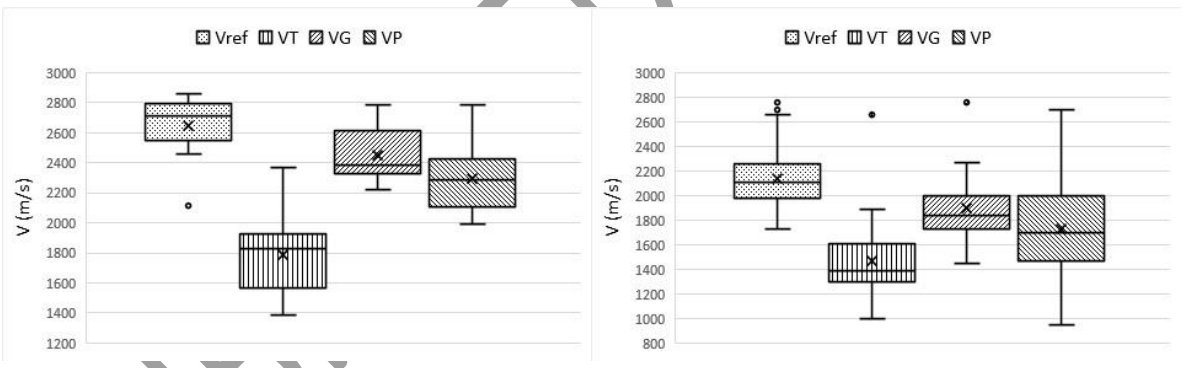

Figure 14. V (m/s) data in specimens with adhesion defects. DT (left) and ST (right). Vref = V in reference specimens without defects, VT = V in correspondence with Teflon, VG = V in correspondence with Glue, VP = V in correspondence with Plastic.

From Tables 6 and 7 and from the plots in Figure 14, the presence of defects determines, with respect to the reference specimens without defects, a decrease in V different according to the type of defect considered. This is confirmed by the application of the Mann-Whitney U test, reported in Tables 8 and 9, which gives the probability of rejecting the null hypothesis.

Table 8. Probability of rejecting the null hypothesis of Mann-Whitney U test for V difference between non-defective and defective specimens. Significance level p = 0.05. U is compared to critical value U* at p < 0 .05. U* = 216 for DT measurements and = 864 for ST measurements.

	Vref vs VT		Vref vs VG		Vref vs VP	
	DT	ST	DT	ST	DT	ST

Mann-Whitney U test	5.5<216	57<864	88.5<216	387.5<864	54<216	307<874

Table 9. Probability of rejecting the null hypothesis of Mann-Whitney U test for V difference between paths running into different defects. Significance level p = 0.05. U is compared to critical value U* at p < 0 .05. U* = 288 for DT measurements and = 1152 for ST measurements.

	VT vs VG		VT vs VP		VG vs VP	
	DT	ST	DT	ST	DT	ST
Mann-Whitney U test	12<288	256<1152	41<288	593.5<1152	157.5<288	798.5<1152

The results reported in Table 8 signify that V data associated with defective and non-defective specimens are extracted from different populations with a probability higher than 95%. Similarly, the results in Table 9 signify that V data associated with paths running into different defects are extracted from different populations with a probability higher than 95%. It is interesting to note that Teflon causes the greatest V decrease - about 32% for DT and 28% for ST -, followed by the plastic - about 13% for DT and 18% for ST -, and finally by the glue, which instead determines the minor decrease - about 7% for DT and 11% for ST (see Table 6). This outcome is consistent with the different acoustic impedance of the materials used to simulate the defects. In the most common databases [54] it is reported that Teflon has a lower acoustic impedance than the other materials involved in the experiment, and for this reason it is frequently used for the simulation of adhesion defects at the interface between FRC and substrate. The sensitivity of UPV, both in DT and ST modes, to the different type of defect is a result worthy of further investigation, as the technique could be used both to identify the presence of adhesion defects and to discriminate the type of defect.

5. Limits of application

The results previously explained point out that UPV allows to identify the presence of adhesion defects and evoke the possibility of discriminating between different defects both when using DT and ST. Therefore, also the ST method is effective in this type of investigation, and this is especially interesting since the DT often cannot be used due to the impossibility of accessing opposite surfaces of the structural element.

However, there are some aspects, listed below, that need to be further explored to confirm the effectiveness of the proposed approach, especially in on-site applications.

In the herein experiment, the acquisitions of ultrasonic signals are made by setting the emitter transducer in correspondence with the defect, whose position is known. On the one hand, this allows to evaluate the effectiveness of the methodology used, on the other, however, it does not necessarily reflect the real situations, in which indeed the position of any defect is not known, but is instead the unknown to be detected. Therefore, it would be appropriate, to test the effectiveness of UPV in on-site investigations, to carry out an experimental campaign in which the position of the transducers is random with respect to the position of the defects. This can be done, for example, by defining a proper grid of measuring points randomly arranged and evaluating the sensitivity of DT and ST in this situation. It should be taken into account that the choice of the measurements grid significantly influences the diagnostic capacity of UPV, and that the proportion between the grid pitch and the size of the defect, along with the

misalignment between the centre of the grid cell and the position of the defect, are very influencing factors [55].

As with all NDT, there are limits beyond which defects cannot be identified by UPV. Generally, these limits depend on the characteristics of the signal (frequency and wavelength). In fact, as a rule, defects smaller than the wavelength of the signal are scarcely or not at all detectable, so high-frequency signals are more sensitive, but less penetrating due to the lower energy, than low-frequency signals. A choice should therefore be made concerning transducers and signals according to the size of the defects to be detected. In the specific case of the adhesion defects between FRC and concrete, to simplify, the problem translates into the definition of the dimensional threshold below which the adhesion defect is considered irrelevant. This very important aspect is still being studied and debated, is addressed in some standards and guidelines [56] and is however outside the scope of this work. In the event of using commercial-type ultrasound equipment, which has piezoelectric transducers with frequencies generally varying between 20 kHz and 500 kHz, it is necessary to establish what is the velocity decrease threshold above which the presence of a defect is supposed. The use of V measurement grids can be useful also for this purpose since they allow the processing of V maps where to identify the position of areas with low V values. The threshold for supposing a defect can be roughly defined by the standard deviation from the average V of the various points of the grid. However, this is certainly an aspect worthy of further study.

6. Conclusions

The results of Ultrasonic Pulse Velocity testing application to detect adhesion defects at the interface between FRP/FRCM and concrete have been reported and discussed. Tests have been carried out on several strengthened concrete specimens in which some artificial adhesion defects have been specifically settled. Both direct and semi-direct ultrasonic measurements have been applied, being the propagation velocity of the ultrasonic signal the analysed quantity. The conclusions can be summarized as follows.

- The velocities of propagation measured with the direct and the semi-direct techniques are appreciably different, with percentage difference in non-defective specimens varying in the range 18%-30% depending on the presence of reinforcement or not. This agrees with the theoretical model that generally acknowledges higher travel time for paths different form the one along the axis of the ultrasonic beam.
- The three types of reinforcements (FRP lamina, FRP sheet, and FRCM sheet) do not have an appreciably different effect on velocity measurements in the context of each measurement method (DT or ST), as highlighted by the U test which discards the hypothesis that the three samples are extracted from one single population with a probability of about 95%.
- The presence of adhesion defects determines, with respect to the reference specimens without defects, a decrease in velocity significantly different, for both direct and semi-direct modes, according to the type of defect considered. Teflon causes the greatest V decrease, about 32% for DT and 28% for ST, followed by the plastic, about 13% for DT and 18% for ST, and finally by the glue, about 7% for DT and 11% for ST. This is consistent with the different acoustic impedances of the materials involved in the experimental test.
- The semi-direct transmission is a testing method as fitting as the direct one in detecting the adhesion defects, and this is particularly interesting since in many real situations the application of direct transmission is prevented.

Further research would be appropriate to confirm the effectiveness of the proposed approach on site, considering the influence of the following important issues.

- The position of the transducers with respect to the defect, perhaps evaluating the sensitivity of DT and ST when a grid of measuring points randomly arranged is settled.
- The size of the defect, whose detectability is affected by the characteristics of the signal, the measurements points arrangements, and the misalignment between the signal path and the position of the defect.
- The velocity threshold that identifies a defect, which could be roughly defined as the standard deviation from the average V of the various signal paths.

Conflicts of Interest

The authors declare that there is no conflict of interest regarding the publication of this paper.

Acknowledgments

The authors would like to acknowledge the financial support of Fondazione di Sardegna (year 2019).

References

1. Mugahed Amran, Y.H.; Rayed, Alyousef; Raizal, S.M. Rashid; Hisham, Alabduljabbar; Chung-Chan Hung. Properties and applications of FRP in strengthening RC structures: A review. *Structures* **2018**, *16*, pp. 208-238.
2. Mallick, P.K. *Fiber-reinforced composites: materials, manufacturing, and design*, 3rd ed.; Taylor & Francis Inc., Publisher Location, Country, 2007; p. 638.
3. Guo, F.; Al-Saadi, S.; Singh Raman, R.K.; Zhao, X.L. Durability of fiber reinforced polymer (FRP) in simulated seawater sea sand concrete (SWSSC) environment. *Corrosion Science* **2018**, *141*, pp. 1-13.
4. Mohammedameen, A.; Gülşan, M.E.; Alzeebaree, R.; Çevik, A.; Niş, A. Mechanical and durability performance of FRP confined and unconfined strain hardening cementitious composites exposed to sulfate attack. *Construction and Building Materials* **2019**, *207*, pp. 158-173.
5. Valdés, M.; Concu, G.; de Nicolo, B. FRP Strengthening of Masonry Columns: Experimental Tests and Theoretical Analysis. *Key Engineering Materials* **2014**, *624*, pp. 603–610.
6. Yu-Fei Wu; Xin-Sheng Xu; Jia-Bin Sun; Cheng Jiang. Analytical solution for the bond strength of externally bonded reinforcement. *Composite Structures* **2012**, *94(11)*, pp. 3232-3239.
7. D'Antino, T.; Pellegrino, C. Bond between FRP composites and concrete: Assessment of design procedures and analytical models. *Composites Part B: Engineering* **2014**, *60*, pp. 440-456.
8. Iovinella, I.; Prota, A.; Mazzotti C. Influence of surface roughness on the bond of FRP laminates to concrete. *Construction and Building Materials* **2013**, *40*, pp. 533-542.
9. Bastianini, F.; Di Tommaso, A.; Pascale, G. Ultrasonic Nondestructive assessment of bonding defects in composite structural strengthenings. *Composite Structures* **2001**, *53(4)*, pp.463-467.
10. Mahmut, E.; Galati, N.; Myers, J.; Nanni, A.; Godinez, V. Acousto-Ultrasonic Technology for Nondestructive Evaluation of Concrete Bridge Members Strengthened by Carbon Fiber-Reinforced Polymer. *Transportation Research Record* **2005**, *1928(1)*, pp. 245-251.
11. Li, J.; Lu, Y.; Guan, R.; Qu, W. Guided waves for debonding identification in CFRP-reinforced concrete beams. *Constr. Build. Mater.* **2017**, *131*, pp. 388–399.
12. Mirmiran, A.; Wei, Y. Damage assessment of FRP-encased concrete using ultrasonic pulse velocity. *Journal of Engineering Mechanics* **2001**, *127(2)*, pp. 126-135.

13. Mahmoud, A.M.; Ammar, H.H.; Mukdadi, O.M.; Ray, I.; Imani, F.S.; Chen, A.; Davalos, J.F. Non-destructive ultrasonic evaluation of CFRP–concrete specimens subjected to accelerated aging conditions. *NDT & E International* **2010**, *43(7)*, pp. 635-641.
14. Dugnani, R.; Zhuang, Y.; Kopsaftopoulos, F.; Chang, F.K. Adhesive bond-line degradation detection via a cross-correlation electromechanical impedance–based approach. *Structural Health Monitoring* **2016**, *15(6)*, pp.650-667
15. La Malfa Ribolla, E.; Hajidehi, M.R.; Fileccia Scimemi, G.; Spada, A.; Giambanco, G. Assessment of bonding defects in FRP reinforced structures via ultrasonic technique. *Challenge journal of structural mechanics* **2016**, *2(3)*, pp. 139–146.
16. La Malfa Ribolla, E.; Hajidehi, M.R.; Rizzo, P.; Fileccia Scimemi, G.; Spada, A.; Giambanco, G. Ultrasonic inspection for the detection of debonding in CFRP-reinforced concrete. *Structure and Infrastructure Engineering. Maintenance, Management, Life-Cycle Design and Performance* **2018**, *14(6)*, pp. 807-816.
17. Concu, G.; De Nicolo, B.; Meloni, D.; Piga, C.; Trulli, N. Infrared thermography and ultrasound techniques for detecting FRP-concrete adhesion problems. Proceedings of the 4th International Conference on Structural Engineering, Mechanics and Computation, Cape Town, South Africa, 6-8 September 2010.
18. Lee, T.; Lee, J. Setting time and compressive strength prediction model of concrete by nondestructive ultrasonic pulse velocity testing at early age. Construction and Building Materials, 2020, 252 (2020) 119027.
19. Trtnik, G.; Gams, M. Ultrasonic assessment of initial compressive strength gain of cement based materials. Cem. Concr. Res. 2015, 67, 148–155.
20. Trtnik, G.; Gams, M. Recent advances of ultrasonic testing of cement based materials at early ages. Ultrasonics 2014, 54, 66–75.
21. Popovics, J.S.; Subramaniam, K.V. Review of ultrasonic wave reflection applied to early-age concrete and cementitious materials. J. Nondestruct. Eval. 2015, 34, 267.
22. Haach, V.G.; Juliani, L.M.; Roz, M.R.D. Ultrasonic evaluation of mechanical properties of concretes produced with high early strength cement. Constr. Build. Mater. 2015, 96, 1–10.
23. Zhao, Y.; Hao, W.; Xu, X. Experimental study of the working stress state of concrete frame structures through ultrasonic testing. Chem. Eng. Trans. 2017, 62, 919–924.
24. Ivanchev, I. Experimental determination of concrete compressive strength by non-destructive ultrasonic pulse velocity method. Int. J. Res. Appl. Sci. Eng. Technol. 2018, 6, doi:10.22214/ijraset.2018.5313.
25. Saleem, M. Assessing the load carrying capacity of concrete anchor bolts using non-destructive tests and artificial multilayer neural network. Journal of Building Engineering 30 (2020) 101260.
26. Hong, S.; Yoon, S.; Kim, J.; Lee, C.; Kim, S.; Lee, Y. Evaluation of Condition of Concrete Structures Using Ultrasonic Pulse Velocity Method. Appl. Sci. 2020, 10, 706. https://doi.org/10.3390/app10020706.
27. Kewalramani, M.A.; Gupta, R. Concrete compressive strength prediction using ultrasonic pulse velocity through artificial neural networks. Autom. Constr. 2006, 15, 374–379.
28. Concu, G.; De Nicolo, B.; Trulli, N; Valdes, M. Estimation of concrete strength and stiffness by means of ultrasonic testing. In Concrete Repair, Rehabilitation and Retrofitting IV; Dehn, F., Beushausen, H.-D., Alexander, M.G., Moyo, P., Eds.; Taylor & Francis Group, London, UK, 2016; ISBN 978-113802843-2.
29. Saleem, M. Evaluating the Pull-Out Load Capacity of Steel Bolt Using Schmidt Hammer and Ultrasonic Pulse Velocity Test. Structural Engineering & Mechanics. 2018, 65. 10.12989/sem.2018.65.5.601.
30. Benmeddour, F.; Villain, G.; Abraham, O.; Choinska, M. Development of an ultrasonic experimental device to characterise concrete for structural repair. Constr. Build. Mater. 2012, 37, 934–942.
31. Moradi, F.; Rivard, P.; Lamarche, C.P.; Kodjo, S.A. Evaluating the damage in reinforced concrete slabs under bending test with the energy of ultrasonic waves. Constr. Build. Mater. 2014, 73, 663–673.
32. Molero, M.; Aparicio, S.; Al-Assadi, G.; Casati, M.J.; Hernández, M.G.; Anaya, J.J. Evaluation of freeze–thaw damage in concrete by ultrasonic imaging. Ndt E Int. 2012, 52, 86–94.
33. Euichul Hwang; Gyuyong Kim; Gyeongcheol Choe; Minho Yoon; Nenad Gucunski; Jeongsoo Nam. Evaluation of concrete degradation depending on heating conditions by ultrasonic pulse velocity. Construction and Building Materials 2018, 171, 511–520.
34. Shah, A.A.; Ribakov, Y. Non-linear ultrasonic evaluation of damaged concrete based on higher order harmonic generation. Mater. Des. 2009, 30, 4095–4102.
35. Antonaci, P.; Bruno, C.L.E.; Gliozzi, A.S.; Scalerandi, M. Monitoring evolution of compressive damage in concrete with linear and nonlinear ultrasonic methods. Cem. Concr. Res. 2010, 40, 1106–1113.

36. Antonaci, P.; Bruno, C.L.E.; Bocca, P.G.; Scalerandi, M.; Gliozzi, A.S. Nonlinear ultrasonic evaluation of load effects on discontinuities in concrete. Cem. Concr. Res. 2010, 40, 340–346.
37. Rucka, M.; Wilde, K. Experimental study on ultrasonic monitoring of splitting failure in reinforced concrete. J. Nondestruct. Eval. 2013, 32, 372–383.
38. EN 12504-4. 2004. Testing concrete- Part 4: Determination of ultrasonic pulse velocity.
39. Turgut, P.; Kucuk, O.F. Comparative relationships of direct, indirect, and semi-direct ultrasonic pulse velocity measurements in concrete. *Russ. J. Nondestruct. Test.* **2006**, *42(11)*, pp. 745-751.
40. Bui, D.; Kodjo, S.A.; Rivard, P.; Fournier, B. Evaluation of Concrete Distributed Cracks by Ultrasonic Travel Time Shift Under an External Mechanical Perturbation: Study of Indirect and Semi-direct Transmission Configurations. *J. Nondestruct. Eval.* **2013**, *32(1)*, pp. 25–36.
41. Benaicha, M.; Jalbaud, O.; Alaoui, A.H.; Burtschell, Y. Correlation between the mechanical behavior and the ultrasonic velocity of fiber-reinforced concrete. *Construction and Building Materials* **2015**, *101, Part 1*, pp. 702-709.
42. Andi, M.; Baehaki; Khadafi, D. Correlation of reinforcement concrete quality based on variations in UPV testing methods. IOP Conference Series: Materials Science and Engineering, 2019, 673, 012043.
43. Ndagi, A.; Umar, A.A; Hejazi, F.; Jaafar, M.S. Non-destructive assessment of concrete deterioration by ultrasonic pulse velocity: A review. Proceedings of Sustainable Civil and Construction Engineering Conference, IOP Conf. Series: Earth and Environmental Science 2019, 357, 012015.
44. Ivanchev, I.; Slavchev, V. Probable compressive strength and modulus of elasticity of concrete, determined by Non Destructive Ultrasonic Pulse Velocity Method (NDUPVM) in different ways of measuring transducers placement. Proceedings of the XXIX International Scientific Symposium Metrology and Metrology Assurance (MMA), Sozopol, Bulgaria, 2019, pp. 1-5.
45. Saleem, M. Study to detect bond degradation in reinforced concrete beams using ultrasonic pulse velocity test method. Structural Engineering and Mechanics. 2017, 64(4), 427-436, DOI:http://dx.doi.org/10.12989/sem.2017.64.4.427
46. NTC18, Norme Tecniche per le Costruzioni D.M. 17.01.2018, Italian Ministry of Infrastructures and Transportation, 2018 (in Italian).
47. Guidelines for evaluating concrete characteristics on site. Superior Council of Public Works, Central Technical Service, Italy, September 2017; (in Italian).
48. Krautkramer, J.; Krautkramer, H. *Ultrasonic testing of materials*, 4th ed.; Springer-Verlag Berlin Heidelberg, 1990.
49. Le prove non distruttive, Associazione Italiana di Metallurgia, AIM Eds.; Milano, February 2013; (in Italian).
50. Jackson, L.B. *Digital Filters and Signal Processing*, Kluwer Academic Publishers, 1995.
51. Hinton, Y.L. Problems associated with statistical patter recognition of acoustic emission signals in a compact tension fatigue specimen. National Aeronautics and Space Administration NASA/TP-1999-209351 ARL-TR-1691, 1999.
52. Lim, Y.Y.; Smith, S.T.; Soh, C.K. Wave propagation based monitoring of concrete curing using piezoelectric materials: Review and path forward. *NDT & E International* **2018**, *99*, pp.50-63
53. Boulay, C.; Staquet, S.; Azenha, M.; Deraemaeker, A.; Crespini, M.; Carette, J.; Granja, J.; Delsaute, B.; Dumoulin, C.; Karaiskos, G. Monitoring elastic properties of concrete since very early age by means of cyclic loadings, ultrasonic measurements, natural resonant frequency of composite beam (EMM-ARM) and with smart aggregates. Proceedings of the 8th International Conference on Fracture Mechanics of Concrete and Concrete Structures, FraMCoS 2013, 10-14 March 2013, Toledo, Spain.
54. NDT Resource Center. Available online: https://www.nde-ed.org/GeneralResources/MaterialProperties/UT/ut_matlprop_plastics.htm (accessed on 10 July 2020).
55. Concu, G.; Trulli, N. Concrete Defects Sizing by Means of Ultrasonic Velocity Maps. *Buildings* **2018**, *8(12)*, 176.
56. CNR-DT 200 R1/2013, Istruzioni per la Progettazione, l'Esecuzione ed il Controllo di Interventi di Consolidamento Statico mediante l'utilizzo di Compositi Fibrorinforzati, National Research Council, 2013 (in Italian).